Palaeontologia Electronica
palaeo-electronica.org

Morphometric investigation of *Tribrachidium* from Nilpena Ediacara National Park, South Australia

Tory L. Botha, Mary L. Droser, Diego C. García-Bellido, and Emma Sherratt

ABSTRACT

Nilpena Ediacara National Park (South Australia) preserves over 200 specimens of *Tribrachidium heraldicum* and 95 specimens of the newly described *Tribrachidium gehlingi* within the fossiliferous Ediacara Member. We use rotational geometric morphometrics to quantify the morphological variation within each species and the differences between the two. Both species were found to be morphologically different from one another, forming distinct groups within the morphospace. Analysis of the symmetric and asymmetric shape components revealed that both species present limited deformation, suggesting they consisted of a fairly resistant material. Growth appears to have been comprised of various interacting allometric relationships that maintain a consistent overall morphology for both species, possibly constrained by its suspension feeding mode.

Tory L. Botha. School of Biological Sciences, Faculty of Sciences, Engineering and Technology, University of Adelaide, North Terrace, Adelaide, South Australia, Australia. tory.botha@adelaide.edu.au
https://orcid.org/0000-0002-2519-9365
Mary L. Droser. Department of Earth and Planetary Sciences, University of California at Riverside, Riverside, California, USA. droser@ucr.edu
https://orcid.org/0000-0001-7112-5669
Diego C. García-Bellido. School of Biological Sciences, Faculty of Sciences, Engineering and Technology, University of Adelaide, North Terrace, Adelaide, South Australia, Australia and Earth Sciences Section, South Australian Museum, North Terrace, Adelaide, South Australia, Australia. diego.garcia-bellido@adelaide.edu.au
https://orcid.org/0000-0003-1922-9836
Emma Sherratt. School of Biological Sciences, Faculty of Sciences, Engineering and Technology, University of Adelaide, North Terrace, Adelaide, South Australia, Australia.
emma.sherratt@adelaide.edu.au
https://orcid.org/0000-0003-2164-7877

Keywords: Ediacaran; *Tribrachidium*; South Australia; morphology; growth

Submission: 5 February 2024. Acceptance: 1 July 2024.

Final citation: Botha, Tory L., Droser, Mary L., García-Bellido, Diego C., and Sherratt, Emma. 2024. Morphometric investigation of *Tribrachidium* from Nilpena Ediacara National Park, South Australia. Palaeontologia Electronica, 27(2):a36.
https://doi.org/10.26879/1374
palaeo-electronica.org/content/2024/5263-morphology-of-tribrachidium

INTRODUCTION

The Ediacara Biota is a suite of globally distributed fossils that record the first complex, multicellular life in Earth's history. Organised into three assemblages (Avalon, White Sea and Nama), the Flinders Ranges of South Australia preserves the most taxonomically and morphologically diverse of these assemblages, the White Sea (Droser et al., 2015; Coutts et al., 2016; Droser et al., 2019). These fossils occur within the Ediacara Member of the Rawnsley Quartzite across the Flinders Ranges, with the richest occurrence at Nilpena Ediacara National Park (NENP) (Figure 1). Host to approximately 40 described genera, palaeobiological and ecological studies have shed light on feeding modes (Rahman et al., 2015; Gibson et al., 2019, 2021; Cracknell et al., 2021), reproduction (Droser and Gehling, 2008; Hall et al., 2015; Mitchell et al., 2015), growth (Evans et al., 2017; Dunn et al., 2018) and life histories (Mitchell et al., 2015; Boan et al., 2023) for a number of these taxa. Despite this, several taxa remain enigmatic, such as *Tribrachidium heraldicum* and the newly described *Tribrachidium gehlingi*.

Tribrachidium occurs as triradial, circular, hyporelief fossil moulds with diameters ranging from 3–50 mm. The three raised arms radiate from the centre and curve anticlockwise, tapering towards the edge of the organism. Fine lines are also rarely preserved at the margin. *T. heraldicum* is found in both South Australia and Russia, and is characterised by the three main, curved arms with small, convex bullae found connected to their associated arm (Figure 2A–E). *T. gehlingi* has only been found at NENP and differs from *T. heraldicum* in that the three main arms are shorter and less curved, with three secondary arms replacing the bullae which extend over half the length of the main arms (Figure 2E–I). Considered a benthic, sessile organism, recent ecological studies have hypothesised that *T. heraldicum* was an ecological generalist and likely had a seasonal or opportunistic sexual reproduction method due to aggregation of specimens on preferred surfaces (Hall et al., 2015; Boan et al., 2023).

In this study, we quantitatively examine the morphology of the two species using rotational geometric morphometrics (Savriama, 2018). We consider the potential for morphological change of *Tribrachidium heraldicum* across different facies within the Ediacara Member and the morphological differences between *T. heraldicum* and *T. gehlingi*. For both species, patterns of asymmetry are exam-

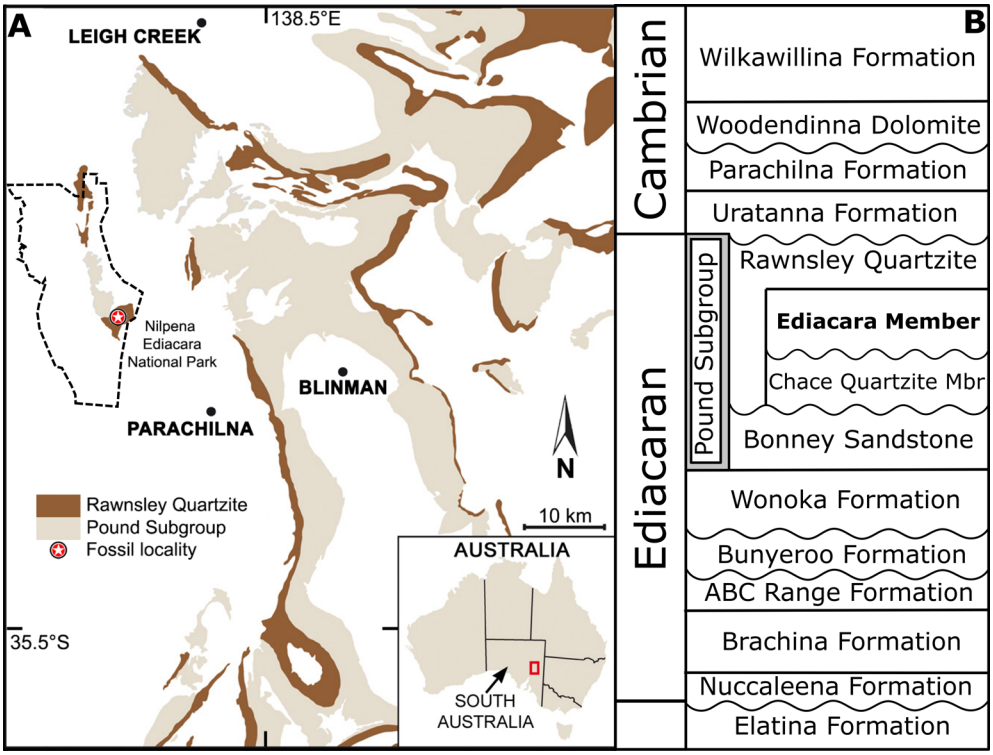

FIGURE 1. Map indicating the location of Nilpena Ediacara National Park (NENP) (A), Flinders Ranges, South Australia, the Pound Subgroup and Rawnsley Quartzite which contains the fossiliferous Ediacara Member (B). A and B modified from Gehling and Droser (2009).

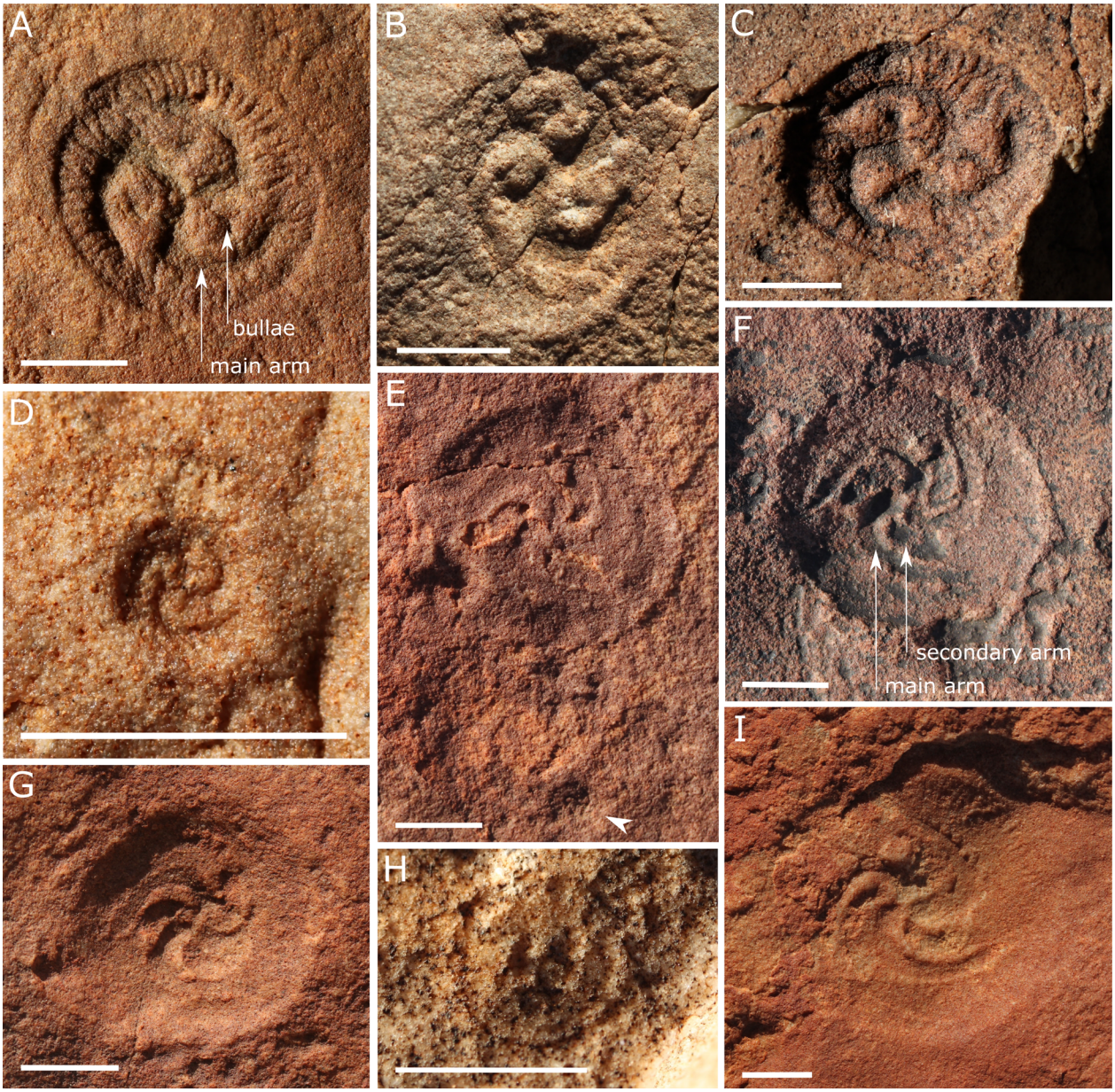

FIGURE 2. *Tribrachidium heraldicum* (A–E) and *T. gehlingi* (E–I) from Nilpena Ediacara National Park (NENP), Flinders Ranges, South Australia. A: SAMA P12898 (Holotype), B: WS-TBEW 108S 149E, C: SAMA P12889 (Paratype), D: LV-Eo Bed 264S 173E, E: F34 *T. heraldicum* (indicated by white arrowhead) and *T. gehlingi*, F: SAMA P59794 (Holotype), G: SAMA P59796 (Paratype), H: SAMA P59800 (Paratype), I: F18. Scale bars equal 10 mm.

ined to understand how overall shape is altered by burial conditions. Following these, shape change with size is assessed to infer how they grew.

GEOLOGICAL SETTING

The Flinders Ranges of South Australia holds an exceptional succession of exposed Neoproterozoic-aged rocks (Figure 1A). A high diversity of Ediacaran fossils is preserved within the Ediacara Member of the Rawnsley Quartzite, which varies in thickness from 10–300 m (Droser et al., 2019; Gehling, 2000) (Figure 1B). The presence of widespread organic mats across the sea floor (Gehling and Droser, 2009; Droser et al., 2022) resulted in the unique sedimentology and preservation of the Ediacara Member and facilitated the excavation and reconstruction of over 33 fossiliferous bedding planes totalling more than 350 m^2 of Ediacaran seafloor at NENP (Tarhan et al., 2017; Droser et al., 2019; Boan et al., 2023). At NENP, fossils of

the Ediacara Biota primarily occur in four facies: Flat-Laminated to Linguoid-Rippled Sandstone (FLLRS), Oscillation-Rippled Sandstone (ORS), Planar-Laminated and Rip-Up Sandstone (PLRUS), and Channelized Sandstone and Sand-Breccia (CSSB) (Gehling and Droser, 2013; Droser et al., 2017; Tarhan et al., 2017; Reid et al., 2018; Droser et al., 2019).

Tribrachidium heraldicum occurs in both the ORS and PLRUS facies, which are interpreted to have been deposited between fair-weather and storm wave base, and sub-wave base upper canyon-fill (respectively) (Gehling and Droser, 2013; Hall et al., 2015; Tarhan et al., 2017; Boan et al., 2023). Specimens are found on 12 fossil beds ranging from a single specimen to over 100 (Hall et al., 2015; Boan et al., 2023) as well as float material (Figure 2A–E). *T. heraldicum* is found in particularly high abundance on two fossil beds: 1T-T and WS-TBEW, which occur in the ORS and PLRUS facies (respectively), each displaying different assemblages of taxa and textured organic surface (TOS) (Droser et al., 2019). The abundance of *T. heraldicum* in both environments suggests that it was ecologically a generalist (Hall et al., 2015). The recently described *Tribrachidium gehlingi* (Figure 2E–I) are predominantly documented from float material on Boomerang Hill, 1.5 km NE of the original Tennis Courts, with a presence on 1T-T, both falling within the ORS facies (Botha and García-Bellido, 2024). Both species are preserved as negative hyporelief external moulds on the bases of sandstone beds (Figure 2), with the presence of concentric forms, interpreted as the underside of *T. heraldicum*, preserved as both negative (transported) and positive (in situ) hyporelief external moulds (Hall et al., 2015; Boan et al., 2023). Additionally, all specimens of both species are associated with bedding surfaces with high Mat Maturity Indexes (MMIs) of 3–4 (Droser et al., 2022).

MATERIAL AND METHODS

Specimens from NENP and the South Australian Museum–Adelaide (SAMA) Palaeontological Collections together comprise over 250 *Tribrachidium heraldicum* and 95 *T. gehlingi*. High resolution three-dimensional (3D) surface scans of *T. heraldicum* and *T. gehlingi* from NENP and the SAMA were taken using the HDI Compact C506 laser scanner (reported accuracy of 12 µm), prepared using FlexScan3D v.3.3 and processed in the MeshLab software v.2022.02 (Cignoni et al., 2008).

Tribrachidium's form was captured using landmark-based geometric morphometrics (Bookstein, 1991; Mitteroecker and Gunz, 2009). Since *Tribrachidium* is a triradial organism, we analysed the landmark data using rotational geometric morphometrics (Savriama, 2018). All landmarked specimens were rotated and relabelled to create three transformed copies (each specimen has three possible configurations; see Figure 3B) using R code provided in Savriama (2018). This method has been applied to another Ediacara organism: *Eoandromeda octobrachiata* (Botha et al., 2023).

All analyses were conducted in the R Statistical Environment v.4.3.1 (R Core Team, 2023) using *Morpho* v.2.9 (Schlager, 2020), *geomorph* v.4.0.1 (Adams et al., 2021), *abind* v.1.4.5 (Plate and Heiberger, 2016), *stats* v.4.3.1 (R Core Team, 2023), and *ggplot2* v.3.4.2 (Wickham, 2016) unless otherwise stated.

Tribrachidium heraldicum: Ediacara Member

To determine whether there was any morphological difference for *T. heraldicum* between facies across the Ediacara Member, specimens from each facies (ORS and PLRUS) were treated as separate populations. SAMA collection specimens were treated as a separate group due to limited locality information. As bullae are not always preserved, to ensure the largest sample size possible, they were not included in the landmarking plan for this dataset (Figure 3). Only 69 specimens were complete enough and available for analysis.

For the aforementioned rotations required, *T. heraldicum* was landmarked in thirds, using the consistent bend in the arms to define the thirds (Figure 3A). The centre was landmarked first, an arm was then captured using two fixed landmarks at each end with five sliding semi-landmarks between, then the corresponding third of the outer rim was landmarked using two fixed landmarks at either end with six sliding semi-landmarks in between. Each third of the specimens were landmarked in a clockwise direction with the relief of the scan as positive (Figure 3B).

Variation due to translation, scale, and rotation was removed from all transformed copies and the original configurations during superimposition using a generalised Procrustes analysis (GPA) using 'procSym' function in *Morpho*. During superimposition, semi-landmarks were permitted to slide along their tangent direction using the minimising bending energy approach (Gunz et al., 2005). A consensus shape was produced by averaging the resulting Procrustes coordinates across all configurations to estimate shape in life (Figure 3C).

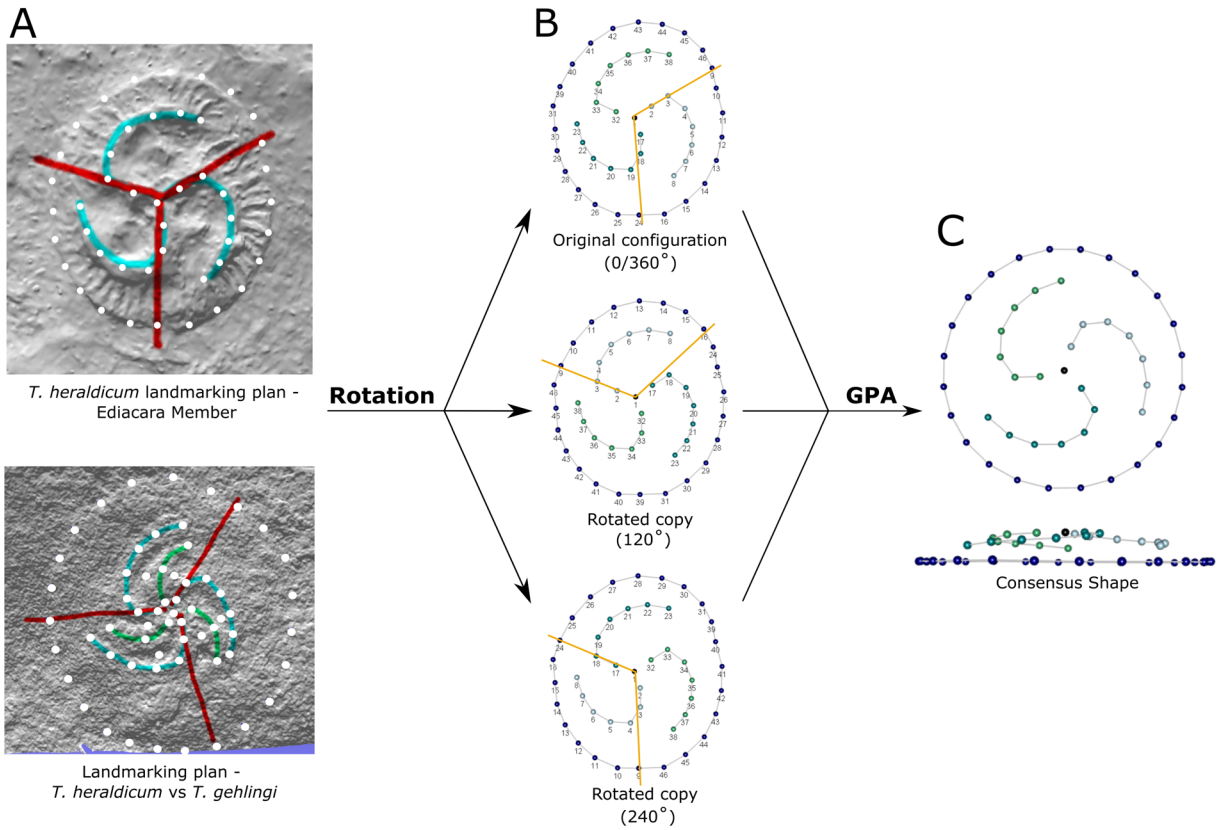

FIGURE 3. Workflow for the shape analysis of the genus *Tribrachidium*. A: Landmarking plans for *T. heraldicum* (SAMA P12898), and for direct comparison of *T. gehlingi* (F43) and *T. heraldicum*. Red lines indicate how thirds are defined for the outer rim, blue lines highlight the arms, green lines highlight the bulla/secondary arms. B: The three rotated copies, orange lines illustrating how the landmarks were rotated. C: Shape configuration graph for the consensus shape for *T. heraldicum*.

To visualise morphological differences of *Tribrachidium heraldicum* across facies from the Ediacara Member, the Procrustes coordinates were ordinated by principal components analysis (PCA) using 'gm.prcomp' function in *geomorph* and visualised in a morphospace. The PCA for rotational geometric morphometrics decomposes the data into symmetric and asymmetric axes. A shape deformation graph for all landmarked specimens was plotted to determine the extent and degree of deformation for *T. heraldicum*.

Tribrachidium gehlingi

Due to the different morphology of *Tribrachidium gehlingi*, the landmarking plan was altered to include the secondary arms as it is a key morphological character (Figure 3A, bottom). The requirement of preserved secondary arms resulted in 38 specimens available for analysis. The landmarking plan implemented for this analysis was like that of *T. heraldicum*, with the inclusion of five landmarks per bulla/secondary arm (BSA) prior to the eight periphery landmarks (Figure 3).

All landmark configurations were subjected to a GPA to obtain the consensus shape to infer shape in life. The Procrustes coordinates were also subjected to a PCA and to visualise the extent and degree of deformation a shape deformation graph was plotted.

Tribrachidium heraldicum vs *T. gehlingi*

To directly compare the two species, 27 specimens of *Tribrachidium heraldicum* were re-landmarked to include the bullae. A PCA was conducted to characterise the morphological differences between the two species and additionally included *T. heraldicum* from Russia. Eight Russian specimens were landmarked from Ivanstov and Zakrevskaya (2021, fig. 3, plates 3 and 4) using ImageJ (Schneider et al., 2012). The landmark coordinates of Australian *T. heraldicum* and *T. gehlingi* were transformed from 3D to 2D using

'pcAlign' function in *Morpho* to account for the 2D nature of the landmarks for the Russian specimens.

Allometry

To infer the patterns of growth for both *Tribrachidium heraldicum* and *T. gehlingi*, the allometric relationship between shape and size was analysed using a two-way analysis of covariance (ANCOVA) model for multivariate data applied with 'procD.lm' function in *geomorph*. The model evaluated included size and species as independent factors, and their interaction. Size was taken as log-transformed centroid size (mm), which is calculated from the landmark coordinates as the square root of the sum of distances of a set of landmarks from their centroid (Bookstein, 1991). This approach allows us to evaluate whether the two species have different allometric growth patterns, and statistical significance is evaluated using permutations (999 iterations). To facilitate species-level comparisons of the allometric patterns, plots of the first principal component of the model's predicted values against size from species-specific regressions were generated (Adams and Nistri, 2010).

Linear measurements were taken to assess the allometric relationships of key morphological elements not captured by the landmarks. Measurements of the arm length, arm distance from the edge, arm width, arm curvature, BSA length, and BSA width were captured using the 'interlmkdist' function in geomorph from the raw landmark coordinates, or measure tool in Meshlab directly on the specimen, and a mean was calculated for each variable per specimen (see Appendix 1). To correct for size, and to retain allometric shape variation, the linear variables were transformed using the log-shape ratios approach (Klingenberg, 2016): each measurement is divided by size (geometric mean of all measurements) and natural logarithm-transformed to obtain the shape variables (Mosimann, 1970; Claude, 2013). To test whether the species differ in allometry in these specific features, two-way ANCOVAs were used to evaluate the relationship between each log-shape ratio and the independent variables log-centroid size and species, and their interaction. These models were also implemented with the 'procD.lm' function in *geomorph* to provide direct comparison with the landmark shape dataset. Finally, simple linear models of the six log-shape ratios vs log-centroid size were performed to calcuate the allometric slope for each species. These were used to assess for each measurement whether they grow by hyperallometry (positive slope values), hypoallometry (negative slope values), or isometry (near zero slope values), as it is for ratios as dependant variables (Klingenberg, 2016). These were implemented with the 'lm' function in *stats* R package.

RESULTS

Tribrachidium heraldicum: Ediacara Member

PCA of the Procrustes residuals produced a total of 132 principal components (PCs). Of these, only the first 20 PCs were used as they describe ~90% of the total shape variation, the remaining are negligible. Of these 20 PCs, 29.9% were symmetrical, and 60.2% asymmetrical (Figure 4A). The mean shape for all landmarked specimens of *T. heraldicum* was symmetrical with arms spiralling in a clockwise direction to the edge with a relatively high relief (Figure 4A).

In a morphospace of the PC axes, complete overlap of specimens from each facies and SAMA collections was observed (Figure 5A).

Tribrachidium gehlingi

The first 24 PCs of the PCA accounted for ~90% of total shape variation. *Tribrachidium gehlingi* had 31.3% symmetrical shape variation, and 59.5% asymmetrical shape variation (Figure 4B).

The mean shape of all landmarked specimens was symmetrical, the three main arms spiral loosely in a clockwise direction leaving a conspicuous rim, with three secondary arms between each main arm extending over half their length and a flat relief (Figure 4B).

Tribrachidium heraldicum vs *T. gehlingi*

Two clear groups corresponding to the two species were observed within the morphospace of the PC axes with no overlap of the 95% confidence intervals. The separation occurred across PC1, with the axis describing a shape change from *Tribrachidium heraldicum* to *T. gehlingi.* High relief, small circular bullae, and arms that spiral close to the edge are observed for *T. heraldicum*, while *T. gehlingi* have a flatter relief, elongate secondary arms, and main arms that do not reach the edge (Figure 5B). This separation and the main shape variation was maintained when the Russian specimens of *T. heraldicum* were added, with them falling in with the Australian specimens of *T. heraldicum*, however, there was some slight overlap in the 95% confidence intervals (Figure 5C).

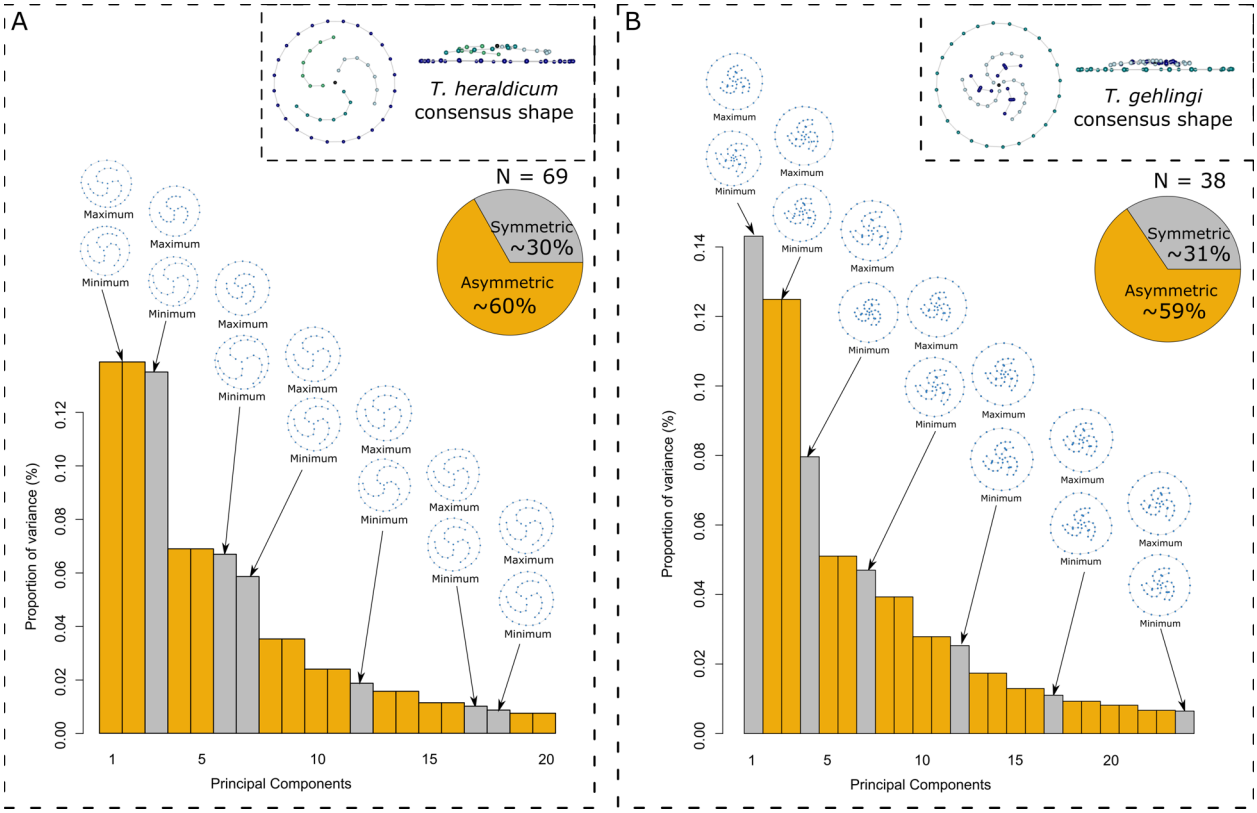

FIGURE 4. Barplot of the principal components that account for ~90% of total shape variation for *Tribrachidium heraldicum* (A) and *T. gehlingi* (B). Symmetric components are identified as single PCs (grey), asymmetrical components (orange) are paired PCs (arranged by the proportion of variance they explain). Shape configuration graphs are given for key PCs, the shape of the minimum and maximum scores for the axis. Pie charts visualising the proportion of symmetrical and asymmetrical components. Shape configuration graphs for the consensus shape for *T. heraldicum* (A) and *T. gehlingi* (B).

Allometry

ANCOVAs of all landmarked specimens revealed species-specific allometric trajectories with only 10.9% of shape change being associated with size (P = 0.001) across both species, 17.9% of shape due to species differences, and an interaction term of size and species also being significant (R^2 = 0.008, P = 0.002) (Table 1). This indicates that *Tribrachidium heraldicum* and *T. gehlingi* at both small and large sizes are distinct in shape, and allometric trajectories are not parallel but remain distinct and do not overlap over the range of sampled sizes (Figure 6A).

Significant linear allometric relationships were found for most features for both species against log-centroid size, including significant interaction terms (Tables 1, 2, Figure 6B–G), indicating species have different growth patterns. Log-mean arm length showed statistically significant allometry for both species and interaction term (Table 1, Figure 6B), and both species exhibited hyperallometry (Table 2). Log-mean arm distance showed significant hypoallometry for *Tribrachidium gehlingi* only (Table 2), with no significant interaction term (Table 1, Figure 6C). No significant relationships were found for log-mean arm width for either species (Table 2, Figure 6D). While *T. heraldicum* showed significant hyperallometry for log-mean curvature, *T. gehlingi* did not (Table 2), however, the interaction term was significant (Table 1, Figure 6E). Log-mean BSA length was also statistically significant for both species (Table 2), with a significant interaction term (Table 1, Figure 6F). Finally, log-mean BSA width was found to be statistically significant for *T. heraldicum*, and not significant for *T. gehlingi* (Table 2), however, there was a significant interaction term (Table 1, Figure 6G).

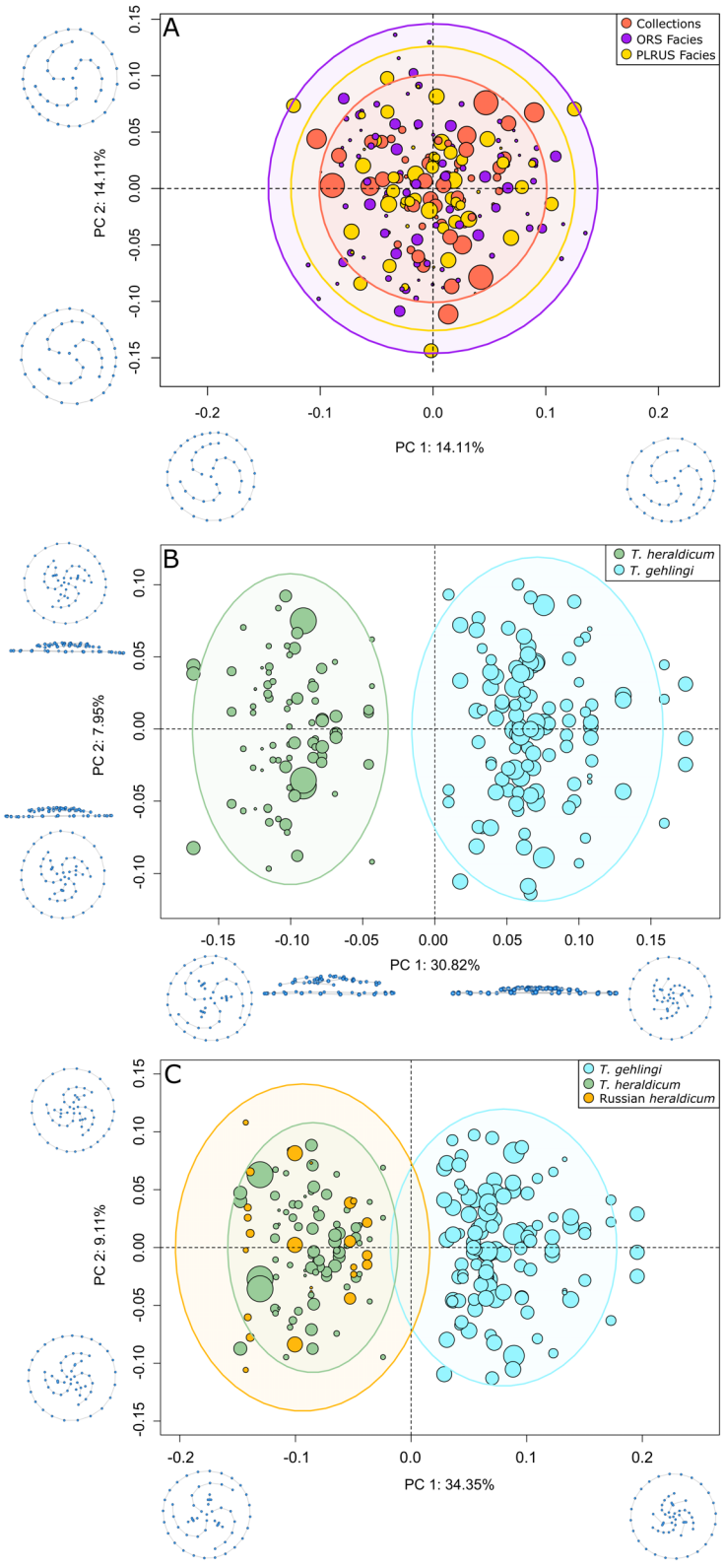

FIGURE 5. Morphospaces of the PC axes for *Tribrachidium heraldicum* across bedding planes in Nilpena Ediacara National Park (A), *T. heraldicum* vs *T. gehlingi* (B), and *T. heraldicum* Australia vs *T. heraldicum* Russia vs *T. gehlingi* (C). Shape configuration graphs are given for the minimum and maximum scores for the axes. Relative size of each specimen is represented by the diameter of each circle. Coloured ellipses represent 95% confidence interval.

TABLE 1. Analysis of covariance results of whole shape derived from landmarks and log-shape ratios of linear variables against independent variables: log-centroid size and species. Model fit (R^2) and P-value obtained by permutations (999 iterations, where alpha = 0.05). Red text indicates non-significant interaction terms.

	R^2	P-Value
landmarked specimens		
Size	0.10954	0.001
Species	0.1794	0.001
Size:Species	0.00881	0.002
log-mean arm length		
Size	0.08686	0.001
Species	0.66167	0.001
Size:Species	0.03709	0.008
log-mean arm distance		
Size	0.09493	0.001
Species	0.6426	0.001
Size:Species	0.01017	0.12
log-mean arm width		
Size	0.19348	0.001
Species	0.20274	0.001
Size:Species	0.02727	0.087
log-mean arm curvature		
Size	0.15114	0.001
Species	0.60204	0.001
Size:Species	0.01729	0.046
log-mean BSA width		
Size	0.29702	0.001
Species	0.17612	0.001
Size:Species	0.07938	0.001
log-mean BSA length		
Size	0.25773	0.001
Species	0.62205	0.001
Size:Species	0.02965	0.001

DISCUSSION

Comparative Morphology

Specimens of *Tribrachidium heraldicum* from the ORS and PLRUS facies of the Ediacara Member overlap in morphospace occupation indicating that there is no significant facies/palaeoenvironmentally controlled morphological differences (Figure 5A). Therefore, the morphology is consistent across different environments including oscillatory currents (ORS) and unidirectional flow (PLRUS). The morphometric comparison of *T. heraldicum* and *T. gehlingi* demonstrated that the two species occupy distinct regions of morphospace (Figure 5B) supporting the findings of a recent qualitative study that established the latter species (Botha and García-Bellido, 2024). When the Russian specimens are included into the analysis, they cluster with the Australian *T. heraldicum* confirming that they are the same species and distinct from *T. gehlingi* (Figure 5C). Individuals of all sizes are found throughout the morphospace, therefore, differences in shape are not driven by allometry, if it were, individuals of similar sizes would be clustered in different areas of the morphospace (Klingenberg, 2016) (Figure 5B, C).

The consistent morphology of *Tribrachidium heraldicum* across environments (between facies) at NENP and with the White Sea, indicate that the triradially symmetrical mean shape produced by the GPA (Figure 4A) is the expected shape in life, after distortion from taphonomy had been eliminated. Although there was a high percentage of asymmetric shape components, when visualised, the extremes of each component do not appear to deviate greatly from the symmetrical mean shape (Figure 4A). Similar to *T. heraldicum*, the triradially symmetrical consensus shape produced by the GPA for *T. gehlingi* is thought to be the shape in life (Figure 4B). Very similar proportions to *T. heraldicum* of asymmetric shape components were observed, when plotted, they also displayed very slight deviation from the symmetrical mean (Figure 4B). Provided the radially symmetrical mean shapes in life for both species, the asymmetry could be interpreted as deformation due to the current at the time of burial, rather than asymmetry in the body plan. The interpretation of asymmetry as a proxy for deformation has been established in Botha et al. (2023) when *Eoandromeda octobrachiata* was shown to have higher proportions of asymmetry on fossil beds with a strongly associated current at the time of burial.

Given the plotted asymmetrical components for both *Tribrachidium heraldicum* and *T. gehlingi* displaying little deviation from symmetry, the level of deformation could be considered low, particularly when compared to certain other taxa present at NENP, such as *Eoandromeda octobrachiata* (Hall et al., 2015; Evans et al., 2019; Botha et al., 2023). Some of these *T. heraldicum* specimens occur in the same facies and sandstone beds as *E. octobrachiata* and were therefore subjected to the same burial event and environment but display much lower levels of deformation (both visually and lower percentage of asymmetrical components),

TABLE 2. Ordinary least-squares linear regression results of log-shape ratios of linear variables. Slope value and P-values of linear models within species. Model values in red indicate non-significant relationships (alpha = 0.05). Red text indicates non-significant regressions.

	Slope Value	P-Value	Allometry
log-mean arm length			
T. heraldicum	0.0704	0.002696	Hyperallometry
T. gehlingi	0.28777	0.0001636	Hyperallometry
log-mean arm distance			
T. heraldicum	-0.13564	0.06793	Isometry
T. gehlingi	-0.30711	0.000193	Hypoallometry
log-mean arm width			
T. heraldicum	-0.08189	0.1736	Isometry
T. gehlingi	0.08706	0.265	Isometry
log-mean arm curvature			
T. heraldicum	0.05787	0.09393	Isometry
T. gehlingi	0.2714	1.07E-02	Hyperallometry
log-mean BSA width			
T. heraldicum	-0.16109	3.74E-03	Hypoallometry
T. gehlingi	0.12632	0.0748	Isometry
log-mean BSA length			
T. heraldicum	-0.15382	0.00127	Hypoallometry
T. gehlingi	0.1745	0.004699	Hyperallometry

indicating that they were somewhat resistant to deformation. A relative flattening of relief with an increase in size was observed in the fossils for *T. heraldicum*, whereas *T. gehlingi* exhibits a consistently flatter relief, which is independent of size (Figure 6A). Given the hypothesised resistance to deformation, the flatter relief of *T. gehlingi* is most likely a biological feature rather than being due to compaction after burial. However, it is uncertain whether the decrease in relief with an increase in size for *T. heraldicum* is a morphological or taphonomic feature. Therefore, it could be suggested that *Tribrachidium* consisted of collagen, enabling them to withstand deformation and maintain shape during compaction (Meyer et al., 2014; Evans et al., 2019).

Several taxonomic affinities have been suggested for *Tribrachidium* based on its morphology including Echinodermata (Paul, 1979), Porifera (Seilacher, 1999; Narbonne, 2005) and Cnidaria (Fedonkin and Cope, 1985; Valentine, 1992). However, recent research into the developmental processes of Ediacaran taxa have placed *Tribrachidium* as a probable stem lineage within Eumetazoa, due to inferred cell type and tissue differentiation, as well as dorso-ventral polarity evident in its morphology (Evans et al., 2021). The overall morphology of *T. heraldicum* presented in this paper supports the hypothesis of a probable stem lineage within Eumetazoa, rather than a specific taxon within Phanerozoic animal clades (Evans et al., 2021). While complex morphological traits are displayed in *Tribrachidium*, there are not enough morphological similarities to confidently assign a more specific taxonomic affinity (i.e., phylum).

With this study, rotational geometric morphometrics has now been applied to three, morphologically distinct, species from the Ediacaran (Botha et al., 2023). This method has successfully enabled patterns of symmetry and asymmetry to be determined to untangle the taphonomy, uncover how they most likely appeared in life, and how they responded to deformation. These results have illustrated that this method is a useful tool for rotationally symmetrical Ediacaran taxa and has the potential to be useful for other species in future.

Growth

As it has been established that there was minimal deformation for both species, the observed allometric variation can be inferred as growth models, with little taphonomic overprint and most likely reflects true shape change with size. Although it is

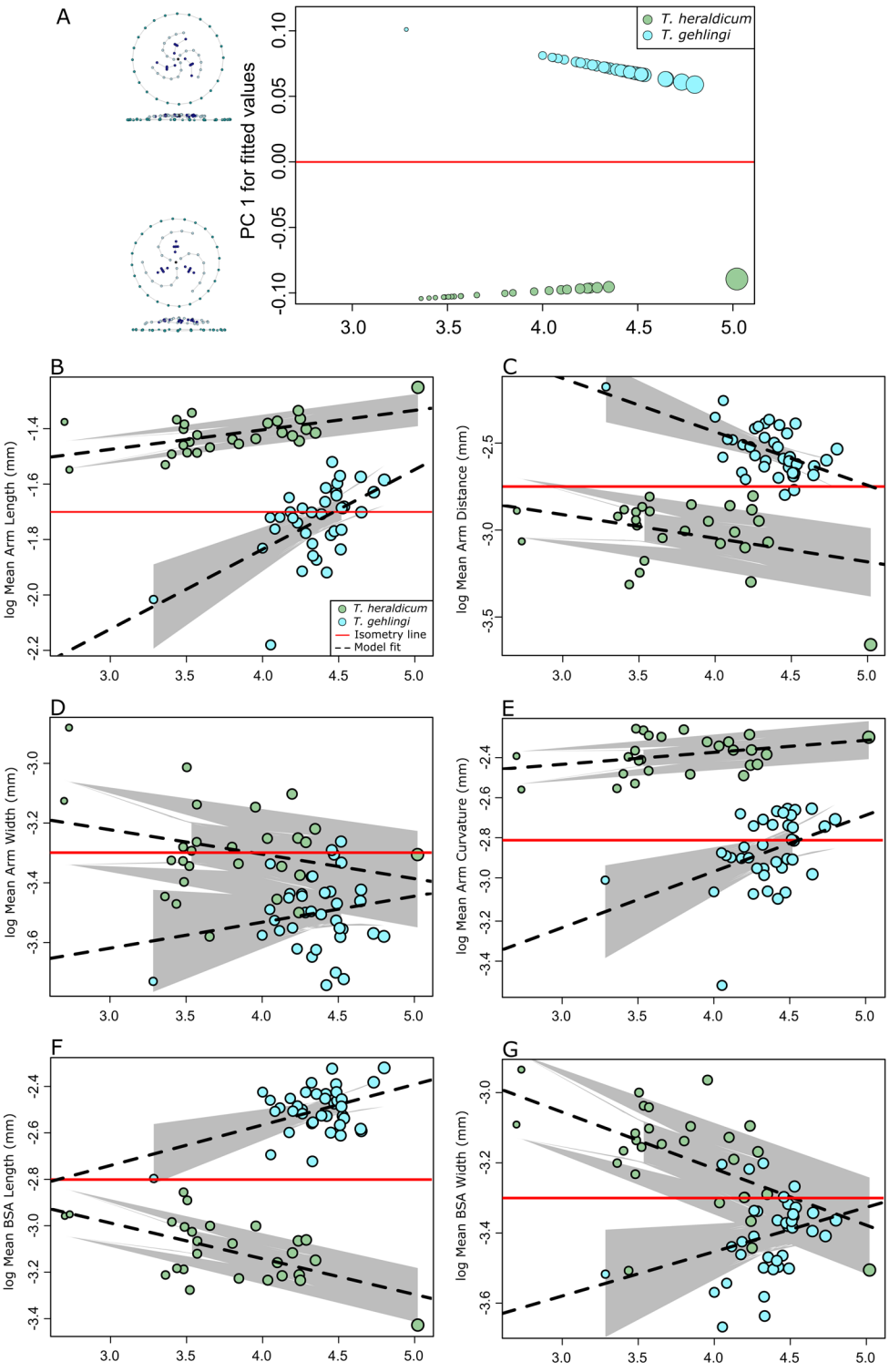

FIGURE 6. Plots investigating shape change with size for *Tribrachidium heraldicum* and *T. gehlingi*. The x-axis for all plots represents log Centroid size and red trendlines demonstrating isometry (slope of 0). A: Multivariate regression of landmark dataset, with size of points proportional to size of the specimen. Shape configuration graphs (left) illustrate the shape each species exhibits throughout growth. B–G: Linear ordinary least-squares regressions of both *Tribrachidium* species. Grey shading illustrates 95% confidence interval of the linear models. B: log mean arm length (mm), C: log mean arm distance (mm), D: log mean arm width (mm), E: log mean arm curvature (mm), F: log mean bulla/secondary arm (BSA) length (mm), G: log mean BSA width (mm).

unknown how large *Tribrachidium* grew, the wide size range for both *T. heraldicum* and *T. gehlingi* (3–50 mm, 10–50 mm, respectively) in this dataset reflects a large enough range to create a reliable growth model. However, as the rate of growth is unknown, size in this case does not relate to age, and thus it is unknown whether the allometric patterns described herein are ontogenetic (across age classes) or static (within an age class) (Klingenberg, 1998).

Results of the ANCOVAs indicate the two species have different size-shape relationships. For whole organismal shape, difference in shape of the two species appears from very small sized individuals. *Tribrachidium heraldicum* presents relatively long main arms and small round bullae, while *T. gehlingi* has shorter main arms with longer secondary arms and a conspicuous rim (Figure 6A). A slight convergence in shape with an increase in size is observed (trends slope towards each other) (Figure 6A), however, an individual from either species would have to be very large before they became the same shape (before the allometric trajectories overlapped), supporting the distinction of these species (Botha and García-Bellido, 2024). Additionally, the sloped nature of the trends further indicates that the overall growth is not isometric for either species, but rather that there are allometric components of their growth (Klingenberg, 2016). Yet, the overall observed shape from the smallest measured individual to the largest (for both species) remains somewhat similar.

The transformed linear measurements provide an insight into the growth patterns of individual morphological features. Majority of the interaction terms were found to be statistically significant (Table 1), thus indicating that both species are displaying different growth patterns, further supporting that the species have different size-shape relationships. Of the tests that were found to be significant ($P < 0.05$), there was a mixture of both hypoallometric relationships (slope < 0) and hyperallometric relationships (slope > 0) (Table 2). The hypoallometric growth for some of the body parts suggests that these features became proportionally smaller as they grew. Hypoallometric growth is common among both vertebrates and invertebrates today (Mirth et al., 2016), appearing in various traits such as the brain (Koh et al., 2005), genitals (Eberhard, 2009), internal organs (Mirth et al., 2016), eyes, and with sexual dimorphism (Werner and Seifan, 2006). Hypoallometry has also been found to be present in the scaling of metabolic rates in vertebrates, where metabolic rate increases at a slower rate than body mass (Kozłowski et al., 2020). Hyperallometric growth suggests that these features grew at a faster rate than the body as a whole. While also common among vertebrates and invertebrates, it typically appears in traits surrounding sexual dimorphism (Tomkins et al., 2005) and reproductive output (Potter and Felmy, 2022). The finding of allometric variation in both species of *Tribrachidium* supports the placement of this genus as a probable stem lineage in Eumetazoa (Evans et al., 2021) and further demonstrates the complexity of these earliest multicellular organisms.

Moreover, it has been long established that the complex forms of multicellular organisms are generated through differential growth of body parts (Huxley, 1932) and are necessary in creating the diversity of morphologies found today (Klingenberg and Froese, 1991; Shingleton and Frankino, 2018). Therefore, it stands to reason that the earliest, complex, multicellular organisms would display differential growth rates to accomplish their relatively diverse forms. Additionally, regulated growth ensures that the relative proportions of morphological traits match final body size and maintain function regardless of any possible environmentally induced variation faced during ontogeny (Gould, 1966; Mirth et al., 2016). Moreover, allometries have been shown that they can evolve to reflect functional and ecological aspects (Adams and Nistri, 2010; Klingenberg, 2010; Wilson and Sánchez-Villagra, 2010) and have been identified as important determinants of constraints on the evolution of shape (Klingenberg, 2010), which is not unreasonable to suggest could be the case for *Tribrachidium* and other Ediacaran taxa. As such, the hypothesised passive suspension feeding mode (Rahman et al., 2015) could have acted as a selection pressure for the regulated growth and shape evolution of *Tribrachidium*, maintaining the functional morphology of their body plans. *T. heraldicum* was found to passively direct water flow and generate lower velocity eddies towards the apex, enabling particles to fall out of suspension (Rahman et al., 2015). Therefore, numerous allometric relationships appear to be interacting to maintain a specific body plan required for the effective nutrient uptake of *Tribrachidium* throughout growth.

Overall, *Tribrachidium heraldicum* and *T. gehlingi* fall in with a growing number of Ediacaran taxa that have been hypothesised to have exhibited regulated growth (Evans et al., 2021) such as *Eoandromeda octobrachiata* (Botha et al., 2023), *Dickinsonia costata* (Evans et al., 2017; Dunn et al., 2018), Rangeomorpha (Hoyal Cuthill and Con-

way Morris, 2014; Dunn et al., 2018), various Dickinsoniomorpha and Erniettomorpha (Dunn et al., 2018), and possibly many other Ediacaran taxa yet to be examined, pushing back the evolution of traits commonly utilised by animals today into the Ediacaran.

CONCLUSIONS

Our study has applied rotational geometric morphometrics on both *Tribrachidium heraldicum* and the newly described *Tribrachidium gehlingi* to better understand their morphology and growth. The results suggest that the morphology of *T. heraldicum* does not change between facies/palaeoenvironments within the Ediacara Member, are consistent between the Australian and Russian specimens, and that it is morphologically distinct from *T. gehlingi*. We observed that *T. heraldicum* and *T. gehlingi* were both resistant to deformation, and thus possibly consisted of a collagen-like material. The addition of another species within the genus *Tribrachidium* illustrates the increasing morphological and taxonomic diversity of the Ediacara Biota. Various allometric relationships within species appear to interact to maintain their different starting morphologies, indicating divergence in early development that is maintained throughout ontogeny. The highly regulated growth of these species could be a constraint on *Tribrachidium* shape due to the functional nature of their body plan in the manipulation of water flow for passive suspension feeding. This demonstrates that even during the early evolution of complex life in the Ediacaran, there were probably many factors influencing and constraining the morphology of these organisms.

DATA AVAILABILITY STATEMENT

Data for this study, including the landmark files, R code (and associated functions), raw measurements, and scan data are available in FigShare: https://doi.org/10.25909/25721535.

ACKNOWLEDGEMENTS

We acknowledge that the Flinders Ranges lie within the traditional lands of the Adnyamathanha people and pay our respect to their Elders past, present and emerging. We would like to thank J. and R. Fargher and the Department of Environment and Water (D.E.W) (permit to DCGB: Q27112-4) for access to the fossils at Nilpena Ediacara National Park. Funding from University of Adelaide Student Support Fund, N. Gary Lane Student Research Award (Paleontological Society), and NASA Exobiology Grants (18-EXO18-0096 and 20-EXO20-0009 to MLD and DCGB) and ARC Discovery Project Grant (DP220102772 to DCGB and MLD). DCGB and ES were supported by Australian Research Council Future Fellowships (FT130101329 and FT190100803 respectively). Additional gratitude to SAMA Palaeontological Collections Manager Dr. M-A Binnie for providing access to specimens in the collections. Thank you to C. Ireland, M-A Binnie, I. Hughes, S. Evans, R. Surprenant and H. McCandless for help and guidance in the field.

REFERENCES

Adams, D. and Nistri, A. 2010. Ontogenetic convergence and evolution of foot morphology in European cave salamanders (Family: Plethodontidae). BMC Evolutionary Biology, 10:216. https://doi.org/10.1186/1471-2148-10-216

Adams, D., Collyer, M., and Kaliontzopoulou, A. 2021. Geomorph: Software for geometric morphometric analyses, Volume R package version 4.0.

Boan, P.C., Evans, S.D., Hall, C.M.S., and Droser, M.L. 2023. Spatial distributions of *Tribrachidium, Rugoconites,* and *Obamus* from the Ediacara Member (Rawnsley Quartzite), South Australia. Paleobiology, 49:601–620. https://doi.org/10.1017/pab.2023.9

Bookstein, F. 1991. Morphometric tools for landmark data. Cambridge University Press, Cambridge, UK, p. 88–124. https://doi.org/10.1017/CBO9780511573064

Botha, T.L., Sherratt, E., Droser, M.L., Gehling, J.G., and García-Bellido, D.C. 2023, Elucidating the morphology and ecology of *Eoandromeda octobrachiata* from the Ediacaran of South Australia. Papers in Palaeontology, 9:e1530. https://doi.org/10.1002/spp2.1530

Botha, T.L. and García-Bellido, D.C. 2024. A new genus of the iconic triradial genus *Tribrachidium*, from Nilpena Ediacara National Park, Flinders Ranges (South Australia). Journal of Paleontology, 98:1–12. https://doi.org/10.1017/jpa.2023.99

Cignoni, P., Callieri, M., Corsini, M., Dellepiane, M., Ganovelli, F., and Ranzuglia, G. 2008. MeshLab: an open-source mesh processing tool. Eurographics Italian Chapter Conference, 1:12–136. https://doi.org/10.2312/LocalChapterEvents/ItalChap/ItalianChapConf2008/129-136

Claude, J. 2013. Log-shape ratios, Procrustes superimposion, elliptical Fourier analysis: three worked examples in R. Hystrix, the Italian Journal of Mammalogy, 24:94–102. https://doi.org/10.4404/hystrix-24.1-6316

Coutts, F.J., Gehling, J.G., and García-Bellido, D.C. 2016. How diverse were early animal communities? An example from Ediacara Conservation Park, Flinders Ranges, South Australia. Alcheringa: An Australasian Journal of Palaeontology, 40:407–421. https://doi.org/10.1080/03115518.2016.1206326

Cracknell, K., García-Bellido, D. C., Gehling, J. G., Ankor, M. J., Darroch, S. A. F. and Rahman, I. A. 2021. Pentaradial eukaryote suggests expansion of suspension feeding in White Sea-aged Ediacaran communities. Scientific Reports, 11. https://doi.org/10.1038/s41598-021-83452-1.

Droser, M.L. and Gehling, J.G. 2008. Synchronous aggregate growth in an abundant new Ediacaran tubular organism. Science, 319:1660–1662 https://doi.org/10.1126/science.1152595

Droser, M.L. and Gehling, J.G. 2015. The advent of animals: The view from the Ediacaran. PNAS, 112:4865–4870. https://doi.org/10.1073/pnas.1403669112

Droser, M.L., Tarhan, L.G., and Gehling, J.G. 2017. The rise of animals in a changing environment: global ecological innovation in the Late Ediacaran. Annual Review of Earth and Planetary Sciences, 45:593–617. https://doi.org/10.1146/annurev-earth-063016-015645

Droser, M.L., Gehling, J.G, Tarhan, L.G., Evans, S.D., Hall, C.M.S., Hughes, I.V., Hughes, E.B., Dzaugis, M., Dzaugis, M., Dzaugis, P., and Rice, D. 2019. Piecing together the puzzle of the Ediacara Biota: excavation and reconstruction at the Ediacara National Heritage site Nilpena (South Australia). Palaeogeography, Palaeoclimatology, Palaeoecology, 513:132–145. https://doi.org/10.1016/j.palaeo.2017.09.007

Droser, M.L., Evans, S.D., Tarhan, L.G., Surprenant, R.L., Hughes, I.V., Hughes, E.B., and Gehling, J.G. 2022. What happens between depositional events, stays between depositional events: the significance of organic mat surfaces in the capture of Ediacara communities and the sedimentary rocks that preserve them. Frontiers in Earth Science, 10. https://doi.org/10.3389/feart.2022.826353

Dunn, F.S., Liu, A.G., and Donoghue, P.C.J. 2018. Ediacaran developmental biology. Biological Reviews, 93:914–932. https://doi.org/10.1111/brv.12379

Eberhard, W.G. 2009. Static allometry and animal genitalia. Evolution, 63:48–66. http://www.jstor.org/stable/25483562

Evans, S.D., Droser, M.L., and Gehling, J.G. 2017. Highly regulated growth and development of the Ediacara macrofossil *Dickinsonia costata*. PloS One, 12:e0176874. https://doi.org/10.1371/journal.pone.0176874

Evans, S.D., Huang, W., Gehling, J.G., Kisailus, D., and Droser, M.L. 2019. Stretched, mangled and torn: responses of the Ediacaran fossil *Dickinsonia* to variable forces. Geology, 47:1049–1053. https://doi.org/10.1130/G46574.1

Evans, S.D., Droser, M.L., and Erwin, D. 2021. Developmental processes in Ediacara macrofossils. Proc. R. Soc. B, 288:20203055. https://doi.org/10.1098/rspb.2020.3055

Fedonkin, M. and Cope, J. 1985. Precambrian metazoans: the problems of preservation, systematics, and evolution (and discussion). Phil. Trans. R. Soc. Lond. B Biol Sci, 311:27–45.
https://www.jstor.org/stable/2396968

Gehling, J.G. 2000. Environmental interpretation and a sequence stratigraphic framework for the terminal Proterozoic Ediacara Member within the Rawnsley Quartzite, South Australia. Precambrian Research, 100:65–95.
https://doi.org/10.1016/S0301-9268(99)00069-8

Gehling, J.G. and Droser, M.L. 2009. Textured organic surfaces associated with the Ediacara Biota in South Australia. Earth-Science Reviews, 96:196–206.
https://doi.org/10.1016/j.earscirev.2009.03.002

Gehling, J.G. and Droser, M.L. 2013. How well do fossil assemblages of the Ediacara Biota tell time? Geology, 41:447–450.
https://doi.org/10.1130/G33881.1

Gibson, B.M., Rahman, I.A., Maloney, K.M., Racicot, R.A., Mocke, H., Laflamme, M., and Darroch, S.A.F. 2019. Gregarious suspension feeding in a modular Ediacaran organism. Science Advances, 5:eaaw0260.
https://doi.org/10.1126/sciadv.aaw0260

Gibson, B.M., Darroch, S.A.F., Maloney, K.M., and Laflamme, M. 2021. The importance of size and location within gregarious populations of *Ernietta plateauensis*. Frontiers in Earth Science, 9.
https://doi.org/10.3389/feart.2021.749150

Gould, S.J. 1966. Allometry and size in ontogeny and phylogeny. Biological Reviews, 41:587–640.
https://doi.org/10.1111/j.1469-185X.1966.tb01624.x

Gunz, P., Mitteroecker, P., and Bookstein, F. L. 2005. Semilandmarks in three dimensions, in modern morphometrics in physical anthropology. Edited by D. E. Slice, pp. 73–98. New York: Kluwer Academic/Plenum Publishers.

Hall, C.M.S., Droser, M.L., Gehling, J.G., and Dzaugis, M. 2015. Paleoecology of the enigmatic *Tribrachidium*: New data from the Ediacaran of South Australia. Precambrian Research, 269:183–194.
https://doi.org/10.1016/j.precamres.2015.08.009

Hoyal Cuthill, J. and Conway Morris, S. 2014. Fractal branching organizations of Ediacaran rangeomorph fronds reveal a lost Proterozoic body plan. PNAS, 111:13122–13126.
https://doi.org/10.1073/pnas.1408542111

Huxley, J. 1932. Problems of relative growth. London: Methuen.

Ivanstov, A. and Zakrevskaya, M. 2021. Trilobozoa, Precambrian tri-radial organisms. Paleontological Journal, 55:72–741.
https://doi.org/10.1134/S0031030121070066

Klingenberg, C.P. 1998. Heterochrony and allometry: the analysis of evolutionary change in ontogeny. Biological Reviews, 73:79–123.
https://doi.org/10.1017/s000632319800512x

Klingenberg, C.P. 2010. There's something afoot in the evolution of ontogenies. BMC Evolutionary Biology, 10:221.
https://doi.org/10.1186/1471-2148-10-221

Klingenberg, C.P. 2016. Size, shape, and form: concepts of allometry in geometric morphometrics. Development Genes and Evolution, 226:113–137.
https://doi.org/10.1007/s00427-016-0539-2

Klingenberg, C.P. and Froese, R.J.S.B. 1991. A multivariate comparison of allometric growth patterns. Systematic Zoology, 40:410–419.
https://doi.org/10.2307/2992236

Koh, I., Lee, M.S., Lee, N.J., Park, K.W., Kim, K.H., Kim, H., and Rhyu, I.J. 2005. Body size effect on brain volume in Korean youth. Neuroreport, 16:202–2032.
https://doi.org/10.1097/00001756-200512190-00012

Kozłowski, J., Konarzewski, M., and Czarnoleski, M. 2020. Coevolution of body size and metabolic rate in vertebrates: a life-history perspective. Biological Reviews, 95:139–1417.
https://doi.org/10.1111%2Fbrv.12615

Meyer, M., Elliott, D., Schiffbauer, J.D., Hall, M., Hoffman, K.H., Schneider, G., Vickers-Rich, P., and Xiao, S. 2014. Taphonomy of the Ediacaran fossil *Pteridinium simplex* preserved three-dimensionally in mass flow deposits, Nama Group, Namibia. Journal of Paleontology, 88:240–252.
https://doi.org/10.1666/13-047

Mirth, C.K., Frankino, W.A., and Shingleton, A.W. 2016. Allometry and size control: what can studies of body size regulation teach us about the evolution of morphological scaling relationships? Current Opinion in Insect Science, 13:93–98.
https://doi.org/10.1016/j.cois.2016.02.010

Mitchell, E.G., Kenchington, C.G., Liu, A.G., Matthews, J.J., and Butterfield, N.J. 2015. Reconstructing the reproductive mode of an Ediacaran macro-organism. Nature, 524:343–346.
https://doi.org/10.1038/nature14646

Mitteroecker, P. and Gunz, P. 2009. Advances in geometric morphometrics. Evolutionary Biology, 36:235–247.
https://doi.org/10.1007/s11692-009-9055-x

Monteiro, L. 1999. Multivariate regression models and geometric morphometrics: the search for causal factors in the analysis of shape. Systematic Biology, 48:192–199.
https://www.jstor.org/stable/2585275

Mosimann, J. 1970. Size Allometry: Size and shape variables with characterizations of the lognormal and generalized gamma distributions. Journal of the American Statistical Association, 65:930–945.
https://www.jstor.org/stable/2284599

Narbonne, G.M. 2005. THE EDIACARA BIOTA: Neoproterozoic origin of animals and their ecosystems. Annual Review of Earth and Planetary Sciences, 33:421–442.
https://doi.org/10.1146/annurev.earth.33.092203.122519

Paul, C. 1979. Early echinoderm radiation. Origin of Major Invertebrate Groups, Systematics Association Special Volume 12. Academic Press, London.

Plate, T. and Heiberger, R. 2016. Abind: combine multidimensional arrays, Volume R Package 1.4-5.

Potter, T. and Felmy, A. 2022. An ecological explanation for hyperallometric scaling of reproduction. Functional Ecology, 36:1513-1523.
https://doi.org/10.1111/1365-2435.14045

R Core Team. 2023. R: A language and environment for statistical computing, R Foundation for Statistical Computing.

Rahman, I.A., Darroch, S.A.F., Racicot, R.A., and Laflamme, M. 2015. Suspension feeding in the enigmatic Ediacaran organism *Tribrachidium* demonstrates complexity of Neoproterozoic ecosystems. Science Advances, 1:e1500800.
https://doi.org/10.1126/sciadv.1500800

Reid, L.M., Holmes, J.D., Payne, J.L., García-Bellido, D.C., and Jago, J.B. 2018. Taxa, turnover and taphofacies: a preliminary analysis of facies-assemblage relationships in the Ediacara Member (Flinders Ranges, South Australia). Australian Journal of Earth Sciences, 67:905–914.
https://doi.org/10.1080/08120099.2018.1488767

Savriama, Y. 2018. A step-by-step guide for geometric morphometrics of floral symmetry. Frontiers in Plant Science, 9:1–24.
https://doi.org/10.3389/fpls.2018.01433

Schlager, S. 2020. Morpho and Rvcg — Shape analysis in R, statistical shape and deformation analysis, Academic Press, p. 217–256.
https://doi.org/10.1016/B978-0-12-810493-4.00011-0

Schneider, C., Rasband, W., and Eliceiri, K. 2012. NIH Image to ImageJ: 25 years of image analysis. Nature Methods, 9:671–675.
https://doi.org/10.1038/nmeth.2089

Seilacher, A. 1999. Biomat-related lifestyles in the Precambrian. PALAIOS, 14:86–93.
https://doi.org/10.2307/3515363

Sheets, H. and Zelditch, M. 2013. Studying ontogenetic trajectories using resampling methods and landmark data. Hystrix, the Italian Journal of Mammalogy, 24:67–73.
https://doi.org/10.4404/hystrix-24.1-6332

Shingleton, A.W. and Frankino, W.A. 2018. The (ongoing) problem of relative growth. Current Opinion in Insect Science, 25:9–19. https://doi.org/10.1016/j.cois.2017.10.001

Tarhan, L.G., Droser, M.L, Gehling, J.G, and Dzaugis, M. 2017. Microbial mat sandwiches and other anactualistic sedimentary features of the Ediacara Member (Rawnsley Quartzite, South Australia): Implications for Interpretation of the Ediacaran Sedimentary Record. Palaios, 32:181–194. https://doi.org/10.2110/palo.2016.060

Tomkins, J.L., Kotiaho, J.S. and Lebas, N.R. 2005. Matters of scale: positive allometry and the evolution of male dimorphisms. The American Naturalist, 165:389–402. https://doi.org/10.1086/427732

Valentine, J. 1992. The macroevolution of phyla. In Lipps, J. and Signor, P. (eds.), Origin and early evolution of the Metazoa, Plenum Press, New York, p. 525–548. https://doi.org/10.1007/978-1-4899-2427-8_16

Werner, Y.L. and Seifan, T. 2006. Eye size in geckos: Asymmetry, allometry, sexual dimorphism, and behavioral correlates. Journal of Morphology, 267:1486–1500. https://doi.org/10.1002/jmor.10499

Wickham, H. 2016. ggplot2: Elegant Graphics for Data Analysis. Springer-verlag New York.

Wilson, L. and Sánchez-Villagra, M. 2010. Diversity trends and their ontogenetic basis: an exploration of allometric disparity in rodents. Proc. R. Soc. B., 277:1227–1234. https://doi.org/10.1098/rspb.2009.1958

APPENDIX 1

Schematic illustration of the linear measurements taken of *Tribrachidium*.